CHINESE JOURNAL OF PHYSICS VOL. 49 , NO. 1 FEBRUARY 2011

Thermal Conductivity of Superconducting Bulk Metallic Glasses at Very Low Temperatures

D. Rothfuss,[1] U. Kühn,[2] A. Reiser,[1] A. Fleischmann,[1] and C. Enss[1,*]

[1]*Kirchhoff-Institut für Physik, Universität Heidelberg, INF 227, D-69120 Heidelberg, Germany*

[2]*IFW Dresden, Institut fr Festkörper- und Werkstoffforschung P.O. Box 270016, D-01171 Dresden, Germany*

(Received April 12, 2010)

The low-temperature properties of superconducting metallic glasses are governed by atomic tunnelling states. The heat transport well below the transition into the superconducting state is limited by the resonant interaction of phonons with the tunnelling systems. So far, measurements of the thermal conductivity have been performed on thin amorphous films down to about 100 mK and on bulk metallic glasses to about 1 K. Using a novel non-contact method, we have investigated for the first time the thermal transport of a superconducting bulk metallic glass $Zr_{52.5}Ti_5Cu_{17.9}Ni_{14.6}Al_{10}$ down to about 6 mK, testing the prediction of the tunnelling model and searching for a possible influence of nuclear moments on the heat flow. The observed temperature dependence of the thermal conductivity is in reasonable agreement with the prediction of the tunnelling model.

PACS numbers: 61.43.Dq, 65.60.+a, 66.35.+a

I. INTRODUCTION

Since the landmark discovery of Zeller and Pohl, it is well known that the low temperature properties of amorphous solids differ considerably from those of their crystalline counterparts [1]. The origin of these differences is due to atomic tunnelling systems, which arise in the irregular structure of amorphous solids. The standard tunnelling model provides a phenomenological description for both insulating and metallic glasses [2, 3]. The existence of atomic tunnelling systems in amorphous metals is well established. For reviews of the early work, see [4, 5]. The main difference between insulating and metallic glasses at low temperatures stems from the interaction of the conduction electrons with the atomic tunnelling systems in amorphous metals. This interaction has been studied in detail in acoustic experiments with superconducting glasses, where the influence of conduction electrons was switched on and off by a sufficiently large magnetic field (see for example [6]). Well below the superconducting transition, it was found that the relaxation rate of tunnelling systems is several orders of magnitude larger in the normal state compared to the superconducting state [7, 8]. In addition, it was observed that the density of states of the tunnelling systems is affected by conduction electrons [9]. This can be explained by the renormalization of the tunnelling matrix element due to an electronic polaron effect [10–12].

The thermal properties of insulating and superconducting metallic glasses are quite

similar. The thermal conductivity well below the superconducting transition is determined by the resonant scattering of thermal phonons with tunnelling systems. So far, measurements on thin amorphous films have been carried out down to about 100 mK [13]. The results are in good agreement with the expectation from the tunnelling model. In the last two decades, so-called bulk metallic glasses became available [14]. They are suitable materials to study the properties of tunnelling systems in amorphous metals down to very low temperatures. Recently, the first thermal conductivity measurements have been performed on several bulk metallic glasses down to about 1 K [15–17]. At temperatures above 1 K, the thermal transport mechanism is quite complex and experiments in this temperature range do not allow for a stringent test of the applicability of the tunnelling model.

Some years ago, it was discovered that atomic tunnelling systems in amorphous insulators carrying a nuclear magnetic moment experience a fine splitting of the tunnelling levels [18] and show an unexpected magnetic field dependence of their dielectric properties [19]. In addition, it was predicted that these nuclear magnetic moments influence the thermal transport in these glasses [20]. So far, there has been no experimental evidence for such an effect in amorphous metals.

We have investigated for the first time the heat transport of a bulk metallic glass $Zr_{52.5}Ti_5Cu_{17.9}Ni_{14.6}Al_{10}$ below 1 K down to about 5 mK using optical heating and inductive thermometer read out. This technique was developed to perform heat transport measurements on sample with extremely low thermal conductivity [21]. We discuss the results in terms of the tunnelling model and discuss the possible influence of nuclear magnetic moments.

II. THEORETICAL BACKGROUND

The well-known tunnelling model describes the low energy excitations in glasses by atoms or group of atoms that can tunnel between two adjacent sites that are energetically almost degenerate. It assumes that a tunnelling system can be represented by a double-well potential, consisting of two harmonic wells, separated by a small barrier V. The resulting tunnelling splitting of the ground state is given by $\Delta_0 = \hbar\Omega \exp(-\lambda)$, where $\hbar\Omega$ is an effective ground state energy and λ the so-called tunnelling parameter. In an amorphous structure, the depth of the two wells may differ somewhat, which is accounted by introducing an asymmetry energy Δ. Thus the total energy splitting of a tunnelling system is $E = \sqrt{\Delta_0^2 + \Delta^2}$. A central assumption of the tunnelling model concerns the distribution of the parameters λ and Δ. It assumes that these two parameters are independent of each other and uniformly distributed according to

$$P(\Delta, \lambda)\mathrm{d}\Delta\mathrm{d}\lambda = \overline{P}\mathrm{d}\Delta\mathrm{d}\lambda, \tag{1}$$

where $\overline{P}$ is a constant. Within the framework of the tunnelling model, many low-temperature properties of amorphous solids can be described successfully [22, 23].

The heat transport of superconducting metallic glasses well below the transition temperature T_C should be due to thermal phonons. The kinetic formula for the thermal con-

ductivity $\kappa\frac{1}{3}C_D vl$ can be used to derive the temperature dependence. Here C_D denotes the Debye specific heat, v the transverse sound velocity and l the mean free path of the thermal phonons. For $T \ll T_C$, the mean free path is limited by resonant scattering of phonons by atomic tunnelling systems. For this process, the inverse mean free path is given by

$$l_{\mathrm{res}}^{-1} = \frac{\pi\omega\overline{P}\gamma^2}{\rho v^2}\tanh\frac{\hbar\omega}{2\kappa_B T}, \tag{2}$$

where γ represents the deformation potential of the tunnelling system, ρ the density of the metallic glass and ω the frequency of the phonon resonantly interacting with the tunnelling system. Note that we have omitted here any intensity dependence. Using this expression, we can easily derive the temperature dependence of the thermal conductivity. Since the mean contribution to the heat transport stems from thermal phonons with $\hbar\omega \approx 2\kappa_B T$, we may use the approximation $\tanh(\hbar\omega/2\kappa_B T) \approx 1$ to find the temperature dependence of the thermal conductivity to be $\kappa \propto T^2$.

Recently, it has been pointed out, that the temperature dependence of the thermal conductivity may be different if the tunnelling particles carry magnetic quadrupole moments [20]. In this case, three distinct regimes are expected. For temperatures well above the typical quadrupole splitting E_Q for the given glass $T \gg E_Q/\kappa_B$, one expects the original tunnelling model prediction; for temperatures of the order of the quadrupole splitting $T \approx E_Q/\kappa_B$, one should find $\kappa \propto T^p$, with $p < 2$; and for temperatures $T \ll E_Q/\kappa_B$, the phonon thermal conductivity limited by resonant scattering on tunnelling systems will be proportional to T^2, again with a slightly larger prefactor compared to the regime $T \gg E_Q/\kappa_B$. Given the typical quadrupole splitting in metallic glasses, one should expect the transition in the low mK range.

III. EXPERIMENTAL TECHNIQUE

The bulk amorphous $Zr_{52.5}Ti_5Cu_{17.9}Ni_{14.6}Al_{10}$ sample was casted at the IFW Dresden. Master alloy ingots with a weight of 50 g were prepared by melting the pure elements with nominal purities of 99.99 ωt% in an arc furnace. The melting process was realized on a water-cooled copper plate in a Ti-gettered argon atmosphere of 99.9999 ωt% purity. The alloys were re-melted at least three times to achieve homogeneity. In order to achieve the necessary high cooling rates upon solidification, the bulk metallic glass samples were prepared by injection copper mold casting in an argon atmosphere of 99.9999 ωt% purity. The samples were prepared in shape of cylindrical rods with 50-mm length and 3-mm diameter. Finally, X-ray diffraction (XRD) was performed on the sample that verified the vitreous character of the Zr-BMG.

The thermal conductivity measurements were carried out in a ^{3}He/^{4}He-dilution refrigerator in the temperature range from 6 to about 210 mK using a novel non-contact method with one heater and two thermometers [21]. This approach is particularly well suited for thermal conductivity experiments with samples of very small thermal conductance such like superconducting metallic glasses far below T_C. In Figure 1, a schematic

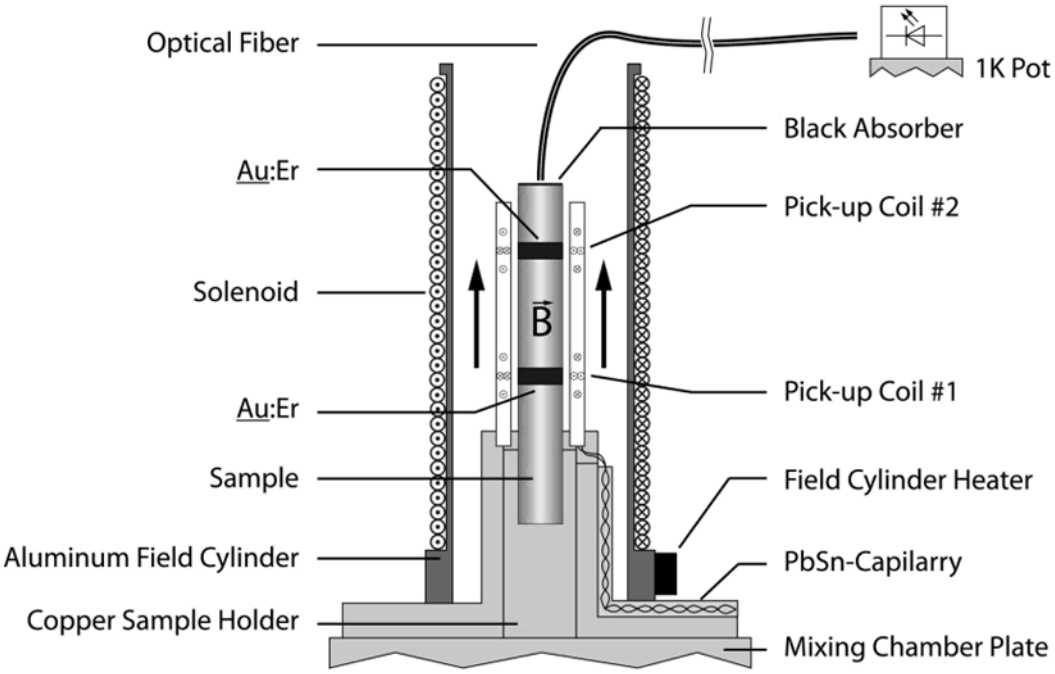

FIG. 1: Schematic diagram of the cylinder-symmetric experimental setup attached to the mixing chamber of a dilution refrigerator. The arrows next to the BMG sample indicate the direction of the applied magnetic field.

diagram of the experimental setup is shown. The metallic glass sample was cut to the length of about 23 mm and has a diameter of 3 mm. Good thermal contact was achieved by clamping one end of the metallic glass to a copper sample holder that was attached to the mixing chamber of the dilution refrigerator, which acted as a constant thermal bath.

A constant heat flow $\dot{Q}$ through the sample was provided by optical heating at the free end of the metallic glass. This was realized by operating a LED (663 nm at 300 K) at the 1-K-Pot of the cryostat and feeding the light though an optical fibre to the sample. To enhance light absorption, on the top end of the sample a thin layer of CuO was deposited. Since the light output of an LED has a nonlinear dependence on the driving voltage, the output was controlled by using a pulsed voltage signal of a constant pulse duration (80 μs) and amplitude (4 V), but with a variable repetition rate v_{rep}. In this way, the heating power can be varied linearly over a very wide range. However, the absolute heat flow through the sample is not known and therefore only the relative change of the thermal conductivity can be measured in our experiment. To determine the absolute value, we plan to perform an additional experiment using a resistive heater to calibrate our LED-based data at the high end of our temperature range. The two thermometers with a distance L apart from each other were situated between the free and the clamped end of the sample and were used to measure the temperature difference ΔTcaused by the heat flow. For small temperature

differences and for steady state condition, the thermal conductivity can be approximated by the linear relation

$$\kappa = \frac{\dot{Q}L}{A\,\Delta T} \propto \frac{v_{\mathrm{rep}}}{\Delta T}, \tag{3}$$

where A is the cross section of the sample perpendicular to the heat flow.

The thermometry is based on the measurement of the magnetization of a paramagnetic material located in a small magnetic field. The paramagnetic sensors used in our experimental setup are made of a dilute alloy of erbium in gold (Au:Er, 750 ppm). The properties of this material have been investigated in recent years in great detail in connection with its applications in micro calorimetry [24–26]. The sensor material was deposed on the cylinder-shaped sample by cathode sputtering as two thin strips with a thickness of 3 μ m, a width of 1 mm, and a centre-to-centre distance of 8.5 mm.

In the limit of a low density of magnetic moments n, the temperature dependence of the magnetization $M(T)$ of a paramagnetic material in an external magnetic field of strength B can be expressed by $M(T) = ngJ\mu_{\mathrm{B}}B_J(x)$, where g denotes the Landé factor, J the total angular momentum of each ion, μ_{B} the Bohr magneton and $B_J(x)$ the Brillouin function with $x = gJ\mu_{\mathrm{B}}B/\kappa_{\mathrm{B}}T$. For small fields and high temperatures, i.e., $x \ll 1$, the expression for $M(T)$ reduces to the Curie law, $M(T) \propto 1/T$. However, the concentration of magnetic ions of temperatures sensors in our experiment were somewhat too high to obey a perfect Curie law in the whole temperature range. We therefore calibrated the magnetization versus temperature relation in situ each measuring cycle as described below.

To monitor the magnetization of the sensors, a small superconducting pick-up coil connected to input coil of a dc-SQUID operating in the flux-locked-loop mode was used. In this way, the resulting flux change at the SQUID is in linear relation with the magnetization of the temperature sensors. As pick-up coils, we used second-order coaxial gradiometers that are sensitive to flux distributions near to the center of the coil, but suppress flux changes, which are constant or have a linear gradient. The gradiometers are made of 125-μm-thick niobium wire and cast in a cylinder of STYCAST 1266 epoxy with an inner diameter of 4 mm, which is placed on a copper holder that is thermally anchored to the mixing chamber. The coils are designed and placed in such way that the corresponding Au:Er sensors are aligned with its centre. In order to avoid pick-up of stray flux, the Nb wires between the pick-up coils and the SQUID input loops are twisted pair wise and shielded by superconducting PbSn capillaries.

To provide a small static magnetic field for the magnetization measurement, the setup is enclosed by an aluminium cylinder onto which a superconducting coil of NbTi is wound. After cooling the mixing chamber well below 1 K, a static field B of about 2 mT oriented along the axis of the sample is generated by applying an appropriate current in the coil and heating the Al cylinder above its critical temperature T_C for a short time. After cooling back down to $T < T_C$ the superconducting cylinder maintains this field when the current is removed.

Figure 2 shows a typical experimental sequence of our measurement at two different temperatures. The change in magnetic flux caused by one of the paramagnetic sensors

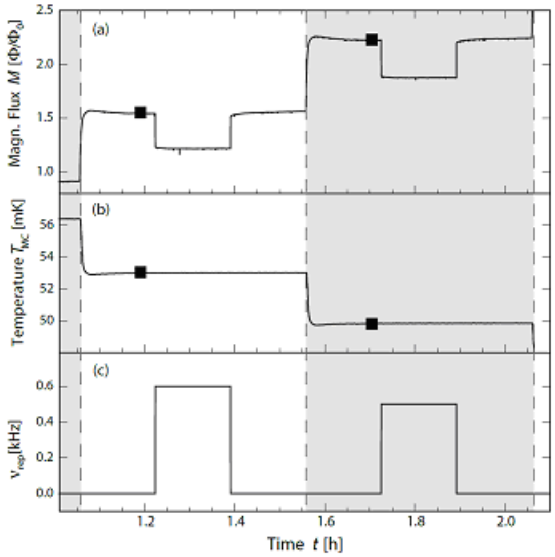

FIG. 2: Measuring sequence. (a) Detected magnetic flux change of one of the paramagnetic sensors, (b) mixing chamber temperature and (c) the repetition rate, which is proportional to the heating power. The black squares mark the points used to calibrate the temperature of the Au:Er sensors.

attached to the sample is shown in (a). Fig. 2(b) displays the variation of the mixing chamber temperature during the same time interval, and Fig. 2(c) the repetition rate of the LED heater. Clearly, the magnetic flux change is correlated with both the mixing chamber temperature and the LED heater. The black squares indicate points that were used to calibrate the paramagnetic sensor. This on-the-fly like calibration has the advantage that it is independent of the knowledge of the exact Au:Er concentration and the applied field and that no pre-calibrated curve is needed.

The measurement is performed for a series of fixed temperatures T_{MC}, with a difference of about 10% between two successive steps. At each step, after the sample is thermalized entirely, i.e., the signal of magnetic flux is constant in time, this value (black squares) and the corresponding temperature of the mixing chamber are taken to generate a temperature calibration of the paramagnetic sensor. As soon as the LED is switched on, constant heat is dissipated into the sample and a thermal gradient develops until a steady state is reached. Finally, the LED is switched off again and the sample cools back to T_{MC} before the next temperature step sequence begins.

IV. RESULTS AND DISCUSSION

Figure 3 shows the result of several individual measurements taken at different temperatures. Displayed are the temperature readings of the mixing chamber thermometer (light grew) and of both paramagnetic temperature sensors attached to the sample (black,

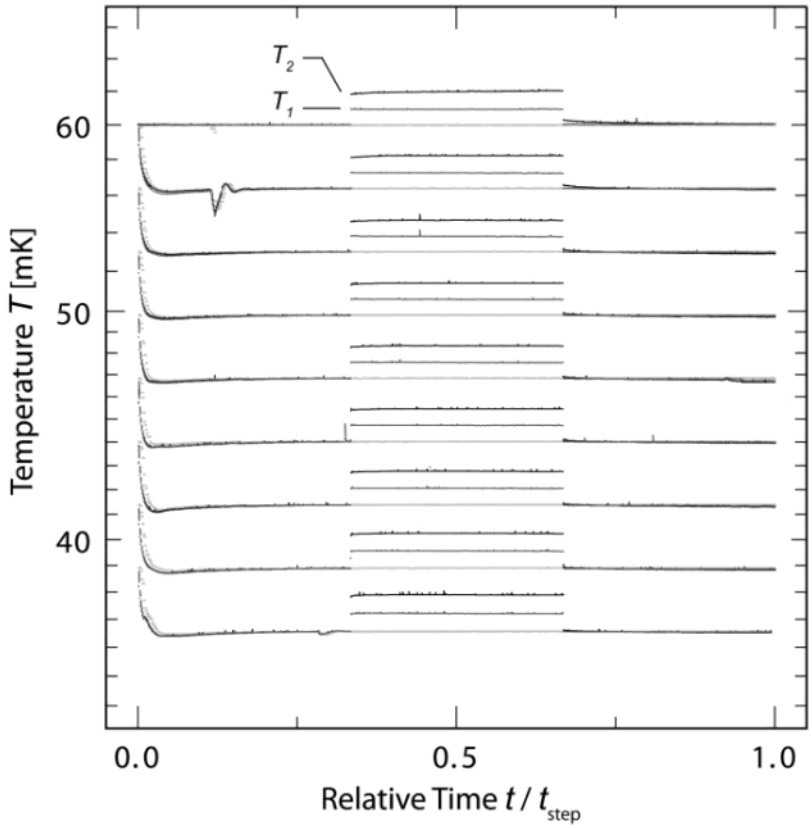

FIG. 3: Temperature of the two paramagnetic Au:Er sensors (black, dark grey) and the mixing chamber thermometer (light grey) as a function of the time normalized to the duration of the temperature steps t_{step}. The label T_2 denotes the temperature reading of the sensor at the upper end of the sample and T_1 the corresponding reading for the sensor closer to the thermal bath.

dark grey) as a function of time normalized with respect to total duration of each temperature step. At the beginning of each curve, one can see the thermalization towards constant mixing chamber temperature after changing the temperature set-point. In the middle part of each temperature step, the heating period is clearly visible. Both sample thermometers react promptly to switching on and off the LED heater. The temperature difference between the two temperature sensors attached to the sample can easily be deduced from these curves.

Together with the known repetition rate, we can derive from these data the relative change of the thermal conductivity as a function of temperature using (3). The result is shown in Figure 4.

These are the first thermal conductivity data obtained for a bulk metallic glass in the millikelvin range and reached for the first time for any amorphous metal below 100 mK. Since the data are taken in a temperature range well below T_c , which is 1030 mK

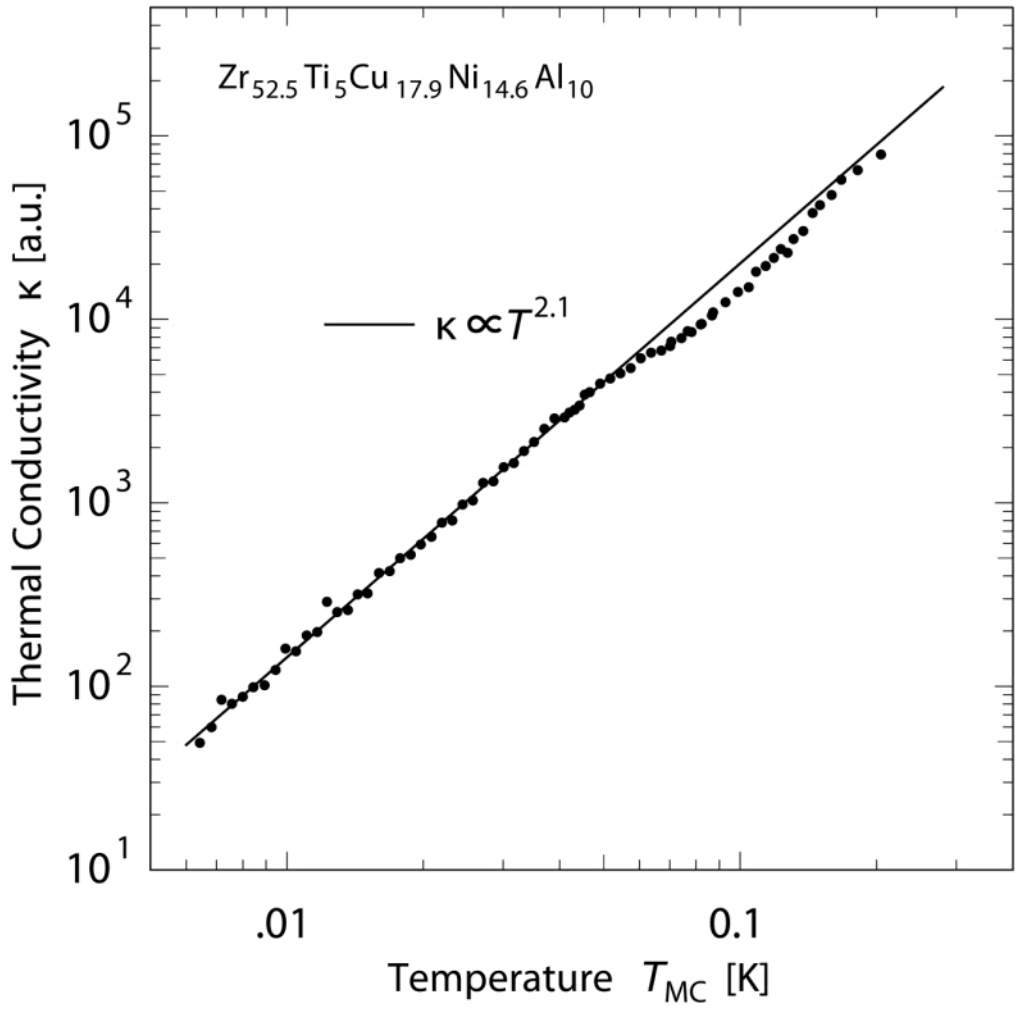

FIG. 4: Temperature dependence of the thermal conductivity of bulk $Zr_{52.5}Ti_5Cu_{17.9}Ni_{14.6}Al_{10}$ in the superconducting state.

for this sample [27], we expect the heat transport to be dominated by thermal phonons. As discussed previously, the mean free path of these phonons should be limited by resonant interaction with atomic tunnelling systems. As pointed out in the theory section the standard tunnelling model predicts a quadratic temperature dependence for this scenario. This seems reasonably well fulfilled at temperatures below about 50 mK, where we find a $\kappa \propto T^{2.1}$ dependence, indicating that the assumption of a uniform distribution of the parameters λ and Δ is valid for tunnelling systems with energies below $\frac{E}{\kappa_B} < 50$ mK.

Above 50 mK, a slight dip with respect to the expected quadratic temperature dependence is observed. At this point, we have no conclusive explanation and can only speculate

about the origin of this finding. One obvious possibility is that the density of states of tunneling systems with energies around 100 mK is somewhat enhanced, in contradiction to the assumption of the tunneling model. An alternative interpretation would be that other kinds of resonantly interacting systems like magnetic moments contribute to the scatting of thermal phonons in this temperature range. Such an interpretation may be tested in thermal conductivity experiments where the sample is driven into the normal-conducting state by a sufficiently high magnetic field.

Finally, we note that we have seen no indication for a possible influence of nuclear magnetic moment, which would be expected to reduce the temperature dependence at very low temperatures. Since we do not know what values the various quadrupole splittings in this sample have, we cannot rule out that the temperature of our experiments was simply not low enough to see such an effect. Clearly, one would need to extend the measurements to temperature below 1 mK to give a definite answer to this question.

V. SUMMARY

For the first time, thermal conductivity of a bulk amorphous metal was measured below 100 mK using a novel non-contact method. The results are in good agreement with the prediction of the standard tunnelling model for superconducting metallic glasses. The origin of the small dip in the temperature of the thermal conductivity compared to the expected value is not clear at this point and will be investigated in further experiments in sufficiently high magnetic fields to drive the sample into the normal state. No indication was found for the influence of nuclear magnetic moments on the heat flow.

Acknowledgments

This work is supported by the European Community—Research Infrastructures under the FP7 Capacities Specific Programme, MICROKELVIN project number 228464. We are thankful for stimulating discussions with M. v. Schickfus, M. Basrafshan, and M. Hempel. We also thank R. Militech for characterising the amorphism of our sample via X-ray diffraction.

References

* Electronic address: christian.enss@kip.uni-heidelberg.de

[1] R. C. Zeller, R. O. Pohl, Phys. Rev. B **4**, 2029 (1971).
[2] P. W. Anderson, B. I. Halperin, C. M. Varma, Phil. Mag. **25**, 1 (1972).
[3] W. A. Phillips, J. Low Temp. **7**, 351 (1972).
[4] J. L. Black, in *Glassy Metals I* (H.-J. Güntherrodt, H. Beck eds.), 167 (Springer, 1981).
[5] H. v. Löhneysen, Phys. Rep. **78**, 161 (1981).
[6] G. Weiss, Mater. Sci. Eng.: A **68**, 45 (1991).

[7] P. Doussineau, P. Legros, A. Levelut, A. Robin, J. Physique Lett. **39**, L-265 (1978).
[8] B. Golding, J. E. Graebner, A. B. Kane, J. L. Black, Phys. Rev. Lett. **41**, 1487 (1978).
[9] H. Neckel, P. Esquinazi, G. Weiss, S. Hunklinger, Solid State Commun. **57**, 151 (1986).
[10] J. Kondo, Physica B **84**, 40 (1976).
[11] Y. Kagan, N. V. Prokofev, JETP Lett. **45**, 116 (1978).
[12] U. Weiss, H. Grabert, S. Linkwitz, J. Low Temp. Phys. **68**, 213 (1987).
[13] R. O. Pohl, X. Liu, E. Thompson, Rev. Mod. Phys. **74**, 991 (2002).
[14] W. H. Wang, C. Dong, C. H. Shek, Mater. Sci. Eng.: R **44**, 45, (2004).
[15] Y. K. Kuo, K. M. Sivakumar, C. A. Su, C. N. Ku, S. T. Lin, A. B. Kaiser, J. B. Qiang, Q. Wang, C. Dong, Phys. Rev. B **74**, 014206 (2006).
[16] Z. Zhou, C. Uher, D. H. Xu, W. L. Johnson, W. Gannon, M. C. Aronson, Appl. Phys. Lett. **89**, 031924 (2006).
[17] Y. Tian, Z. Q. Li, E. Y. Jiang, Solid State Commun. **149**, 1527 (2009).
[18] A. Würger, A. Fleischmann, C. Enss, Phys. Rev. Lett. **89**, 237601 (2002).
[19] P. Strehlow, C. Enss, S. Hunklinger, Phys. Rev. Lett. **80**, 5361 (1998).
[20] A. Akbari, Physica B **403**, 3942 (2008).
[21] H.-Y. Hao, M. Neumann, C. Enss, A. Fleischmann, Rev. Sci. Instr. **75**, 2718 (2004).
[22] *Tunneling Systems in Amorphous Solids*, (P. Esquinazi ed.), (Springer 1999).
[23] S. Hunklinger, C. Enss, in *Insulating and Semiconducting Glasses*, (P. Boolchand ed.), Directions in Condensed Matter Physics Vol. **17**, 499 (World Scientific, Singapore, 2000).
[24] A. Fleischmann, J. Schönefeld, J. Sollner, C. Enss, J. S. Adams, Y. H. Huang, Y. H. Kim, G. M. Seidel, J. Low Temp. Phys. **118**, 7 (2000).
[25] C. Enss, A. Fleischmann, K. Horst, J. Schönefeld, J. Sollner, J. S. Adams, Y. H. Huang, Y. H. Kim, G. M. Seidel, J. Low Temp. Phys. **121**, 137 (2000).
[26] A. Fleischmann, C. Enss, G. M. Seidel, in *Topic of Applied Physics* (C. Enss ed.), **99**, 151 (2005).
[27] D. Rothfuss, *Diploma Thesis*, (Heidelberg University 2008), unpublished.